



African Journal of Biological Sciences



Structural and Dispersion Parameters of Miscible PVA-PAAm-PEG Blend: Effect of carbon nanotubes (CNT)

¹Khansaa Saleem Sharba, ¹Golshad kheiri, ¹Mir Maqsood Golzan, ²Khalid HaneenAbass

¹ Physics Department, Faculty of Science, Urmia University, Urmia, Iran

²Physics department, College of Education for Pure, University of Babylon, Iraq

Corresponding author: pure.khalid.haneen@uobabylon.edu.iq

Abstract

The production of optical instruments, which are in great demand in various fields, expanded to include medical devices. In this study, the polymer is mixed with PVA-PAAm-PEG and different wt.% of CNT nanocomposite films synthesized by the solution casting method resulted in optical microscopy images depicting both feathering and homogeneous dispersion of nanomaterial within the films. The obtained products were identified by scanning electron microscopy (SEM) and showed a powerful dispersion of CNT on the surface of the polymeric matrix. XRD analysis provided confirmation of this observation. the presence of semi-crystalline PVA-PAAm-PEG and CNTs forming square structures aggregated are observed as the weight percent weight of the additive increases up to 20wt.%. Transmittance decreases with increasing CNT concentration, while extinction coefficient dielectric constant (real and imaginary) increases with increasing CNT concentration. This is attributed to increase in electronic polarization in nanocomposite contributed by concentration in films ie. charges within polymers), The study centered on analyzing the single oscillator energy (E_0), static refractive index ($n(0)$), and moments (M_{-1} and M_{-3}).

Keywords: PVA- PAAm-PEG: CNT, cast technique, structural and optical properties.

Article History

Volume 6, Issue 5, 2024

Received: 22 May 2024

Accepted: 29 May 2024

doi:10.33472/AFJBS.6.5.2024.8395-8412

Introduction

In recent years, there has been significant focus on advancing and exploring various polymer blends to enhance material performance. These blends demonstrate unique properties distinct from those of individual polymers, influenced by the compatibility of the base polymers. The adaptability of polymer blends is highly attractive, as their characteristics can be tailored by incorporating different salts and nanoparticles [1,2]. The utilization of block copolymers is a frequently employed technique to improve the structure of immiscible polymer blends. Several experimental studies have shown that block copolymers play a crucial role in reducing the morphology of immiscible blends and improving their stability[3].Therefore, these advancements have captured the attention of scientists and engineers, as they enhance the properties of large polymeric materials for potential commercial applications[4].

Poly (vinyl alcohol) PVA, with the molecular formula $(C_2H_4O)_x$, is classified as a semicrystalline polymer. It is highly regarded as a promising polymer owing to its unique characteristics, such as environmental friendliness, non-toxicity, exceptional water solubility, excellent electrical properties, chemical stability, and favorable optical properties.The hydroxyl groups in PVA enable internal interactions within the polymer composite through hydrogen bonding [5]. PVA is soluble in water and resistant to solvents and oils. Consequently, it finds extensive applications in manufacturing oxygen-resistant membranes in the paper and textile industries. Its melting point is around 230 °C for fully aqueous solutions, 180-190 °C for partially hydrated solutions, and 75-190 °C for the glass transition temperature [6].

Polyacrylamide (PAAm) is a water-soluble polymer with a distinguishing feature of being nontoxic, attributed to its 19.7% nitrogen content [7]. This chemical gel formulation exhibits high water solubility. Its ability to absorb water significantly results in the formation of weakly interconnected crystals, thereby

enhancing the tensile strength of water and strengthening the solution[8]. PAAm is utilized in various applications such as tissue coatings for burns, artificial retinas, and soft tissue, given its properties as a flocculent and material thickener [9].

Polyethylene glycol (PEG) is a versatile polymer with the capacity to exhibit different molecular weights and functions. High molecular weight polyethylene glycol is also known as poly(ethylene oxide) PEO [10]. PEG and PVA share several common properties, including high solubility, low toxicity, biocompatibility, and rapid biodegradability in water [11]; Moreover, both PEG and PVA are characterized by essential functional groups, specifically one hydroxyl group and one carbonyl group per chemical chain [12]. The presence of these functional groups boosts the material's compatibility with a wide range of other polymers, fillers, and nanofillers, making them attractive to scientists, engineers, and researchers striving to modify or enhance material properties[13].

Carbon nanotubes (CNTs) are a distinctive carbon allotrope that manifests as cylindrical tubes constructed from graphite. Recognized for their unique properties, CNTs hold significant promise in the realms of nanotechnology and medicine. Typically measuring in nanometers in diameter and extending a few millimeters in length, these tubes showcase a wide array of electronic, thermal, and structural characteristics. The specific attributes of CNTs, such as their size, length, chirality, and surface properties, govern their diverse range of properties. Particularly noteworthy are their exceptional surface features, hardness, strength, and flexibility, which have garnered significant attention within the pharmaceutical industry[14]. Nanofillers, particularly carbon nanomaterials, consist of very low molecular weight materials embedded within the polymer matrix, resulting in remarkably advanced materials, especially polymer composites of CNT and Graphene, which have garnered significant interest in contemporary science and technology, primarily for their potential applications. When incorporated into polymer matrices [15] graphene can imbue them with distinctive properties.

Notably, graphene has received particular emphasis owing to its exceptional attributes. Derived from natural graphite [16]. Graphene is distinguished as a cost-effective alternative to other fillers, such as CNT [17]. The structures and optical properties of the nanocomposites were investigated (PVA -PAAm -PEG-CNT).

Experimental

Materials

PVA with a molecular weight of 18,000 g/mol and high purity (99.0%) from Panreac in Barcelona, Spain, was synthesized along with PAAm with a molecular weight of 5×10^6 g/mol in high purity (99.99%) obtained from British Drug Houses (BDH) and Reagent World. PEG with a molecular weight of 6000 Dalton and purity of 99.8% in granule form was also used. Additionally, the nanomaterials included varying percentages of CNTs with purity of 90%, a diameter of 100 nm, and a length of 10 μ m. The preparation involved synthesizing PVA-PAAm-PEG:CNT nanocomposites.

preparation of PVA- PAAm-PEG: CNT nanocomposites

The casting method was employed to fabricate nanostructured films of PVA-PAAm-PEG with varying ratios of CNT nanostructures. A total of 2 grams of the polymer was dissolved in 60 mL of water at 90 °C for 1 hour in a beaker to create a PVA-PAAm-PEG mixture consisting of 40% PVA, 40% PAAm, and 20% PEG-PEG-CNT film was then cooled to approximately 25 °C before adding four ratios (0, 0.005, 0.010, 0.015, and 0.020) weight percent of CNT for 1 hour in each case to form PAAm-PVA nanoparticles, as illustrated in Table 1. Subsequently, each of these ratios was dispensed into a Petri dish (5 cm diameter) and allowed to stand for 7 days to enable the solvent to evaporate before gently peeling.

Table1. Summarized the preparation of PVA-PAAm-PEG and PVA-PAAm-PEG: CNT Nanocomposites.

Samples No.	PVA	PAAm	PEG	CNT
1	0.4	0.4	0.2	0.000
2	0.398	0.398	0.199	0.005
3	0.396	0.396	0.198	0.010
4	0.394	0.394	0.197	0.015
5	0.392	0.392	0.196	0.020

Results and Discussions

The morphological characteristics of the PVA-PAAm-PEG blend and the PVA-PAAm-PEG: CNT nanocomposite are portrayed through optical microscopy (OM) images at 100x magnification, as shown in Figures 1. In Figure (a), the polymer mixture displays a smooth surface and homogeneity without any apparent phase separation.

Figures (B, C, D, and E) within the same figure demonstrate the fine diffusion and dispersion of CNT within the blend polymers in the nanocomposites. The dispersion of CNT in the blend appears to be good with fine homogeneity within the samples, and no aggregation of nanoparticles is observed, which is attributed to the interaction among polymers and CNT due to the high surface-to-volume ratio. At a high concentration of 0.020 weight percent of CNT nanotubes, a continuous network of paths is formed through which charge carriers can traverse. This leads to a modification of the material properties, as indicated by the images presented in Figures (B, C, D, and E) [18].

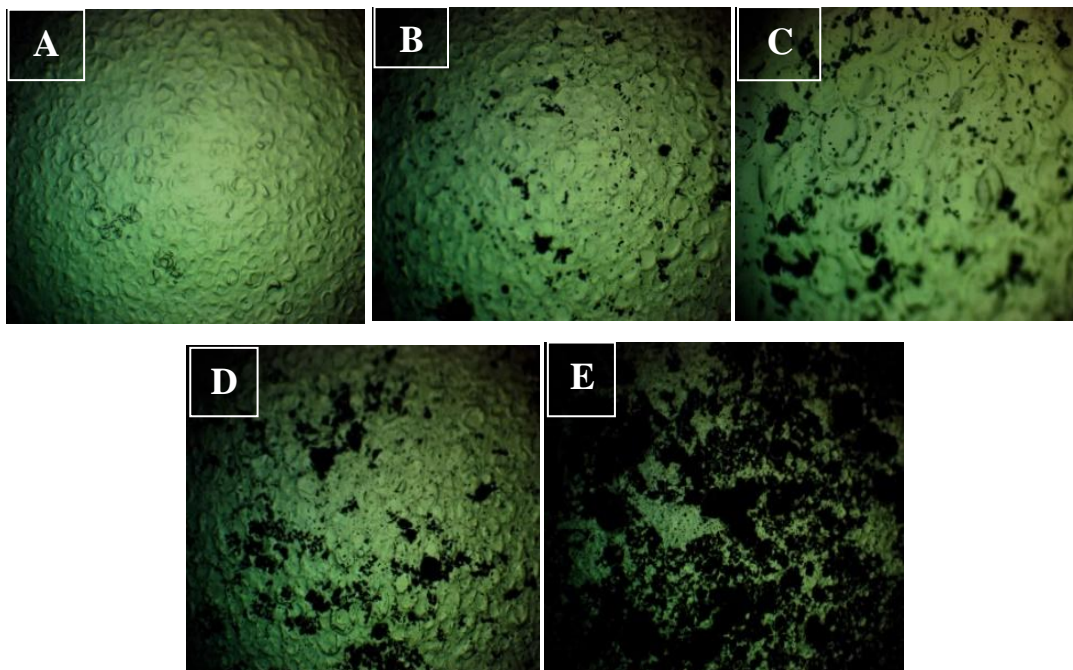


Figure 1. Photomicrographs (100X) of PVA-PAAm-PEG with various content of CNT: (A) 0 wt.% (B) 0.005 wt.% (C) 0.01 wt.% (D) 0.015 wt.% and (E) 0.02 wt.%.

Figure 2 presents an SEM micrograph of the surface of the PVA-PAAm-PEG blend and PVA-PAAm-PEG: CNT nanocomposite films. Images A and B in Figure 2 reveal a uniform morphology with a relatively smooth surface. In figures 2 (C, D, and E), increasing the ratio of CNT in the polymer matrix for the PVA-PAAm-PEG: CNT nanocomposites resulted in changes to the surface morphology and increased roughness. The nanocomposite films exhibit finely dispersed CNT without aggregates, evenly distributed on the surface, suggesting the presence of a homogeneous growth mechanism. In the SEM images, the sizes of CNT particles on the surface of the nanocomposites were measured. The particle sizes of CNT ranged from 339.7 nm in dimensions. These findings are consistent with the optical microscopy images.

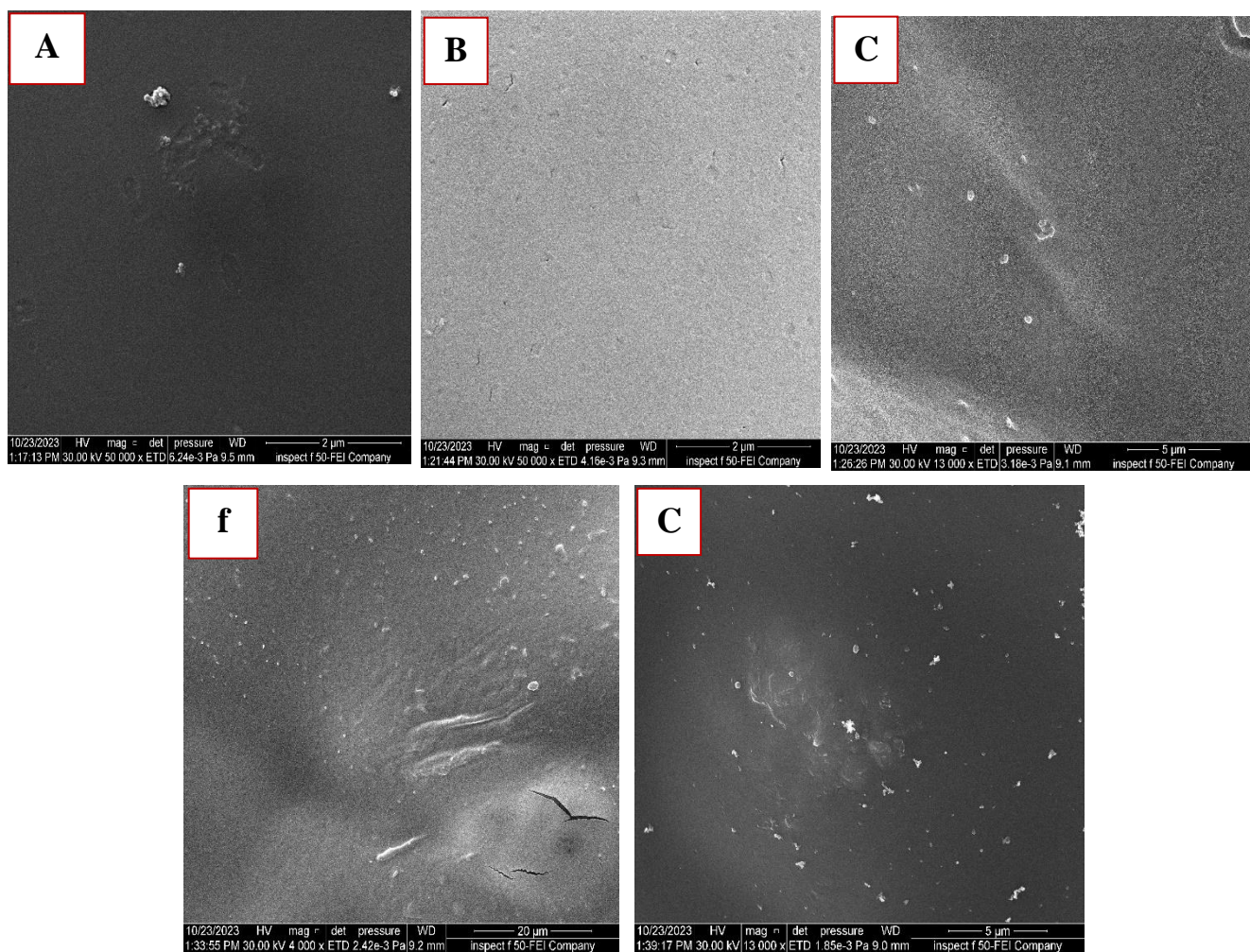


Figure 2. SEM images of PVA-PAAm-PEG: CNT with various content of CNT and magnifications (A) 0 wt.% (B) 0.5 wt.% (C) 1 wt.% (D) 1.5 wt.% and (E) 2 wt.%.

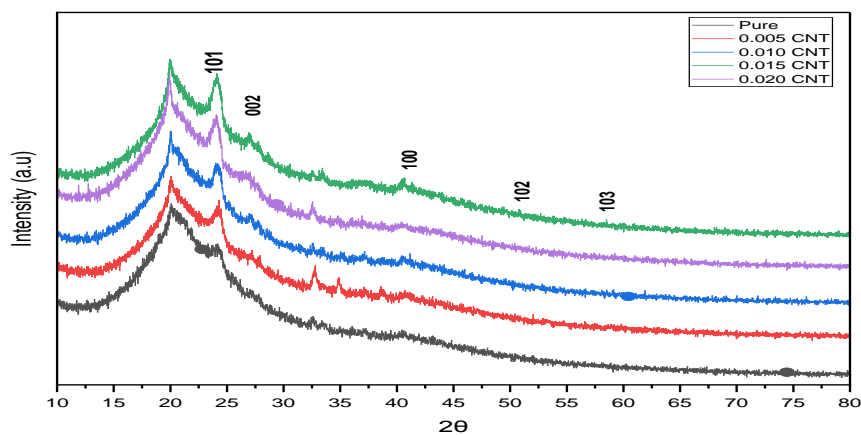


Figure 3. XRD of PVA-PAAm-PEG with various content of CNT: (A) 0 wt.% (B) 0.005 wt.% (C) 0.01 wt.% (D) 0.015 wt.% and (E) 0.02 wt.%.

The crystal structure of PVA-PAAm-PEG: CNT nanocomposites was determined, with the percentage of crystallinity in the pure nanocomposite-blended materials emerging as a crucial physical property. This significance was apparent in the blends of PVA-PAAm-PEG: CNT with varying weight ratios of CNT at room temperature (RT), as shown in Figure 3. X-ray diffraction (XRD) was utilized to analyze the crystallization transition of the pure nanocomposites. The diffraction patterns were obtained by measuring 2θ values ranging from 10° to 80° . The addition of nanoparticles to PVA-PAAm-PEG blends causes a shift in the diffraction peak at $2\theta = 19.88^\circ$ to 23.86° , which is attributed to the (101) reflection plane of semicrystalline PVA. This shift is a result of the hydrogen bonds between PVA molecular chains, indicating the semicrystalline nature of PVA [19]. The XRD spectrum of PVA-PAAm-PEG: CNT nanotubes reveals diffraction peaks at $2\theta = 26.71^\circ$, 41.6° , 50.57° , and 58.92° for the (002), (100), (102), and (103) planes, respectively. These diffraction peaks correspond to the rectangular structure of the CNT particles and are in agreement with the graphite database (JCPDS, Card No.75-1621) [20]. These peaks indicate that the well-dispersed CNTs have been successfully incorporated into the heterogeneous PVA-PAAM-PEG matrix.

Figure 4 illustrates the transmittance spectrum (T) of PVA-PAAm-PEG blend composites with varying concentrations of CNT nanocomposites was measured. The transmittance (T) was determined at room temperature as a function of wavelengths using the following equation [21]:

$$T = I_T / I_o \quad (1)$$

where I_T is the intensity of the radiation leaving the film and the intensity of the radiation incident on the film I_o . The decrease in transmittance spectra with increasing weight percentage of CNTs can be attributed to their addition. The CNTs absorb electrons on the surface, resulting in a decrease in transmission. In the case of the pure film, its message is enhanced. The absence of particles

indicates a lack of free electrons, which necessitates a substantial amount of energy to break bonds during transition. These findings align with those reported by a previous researcher [22].

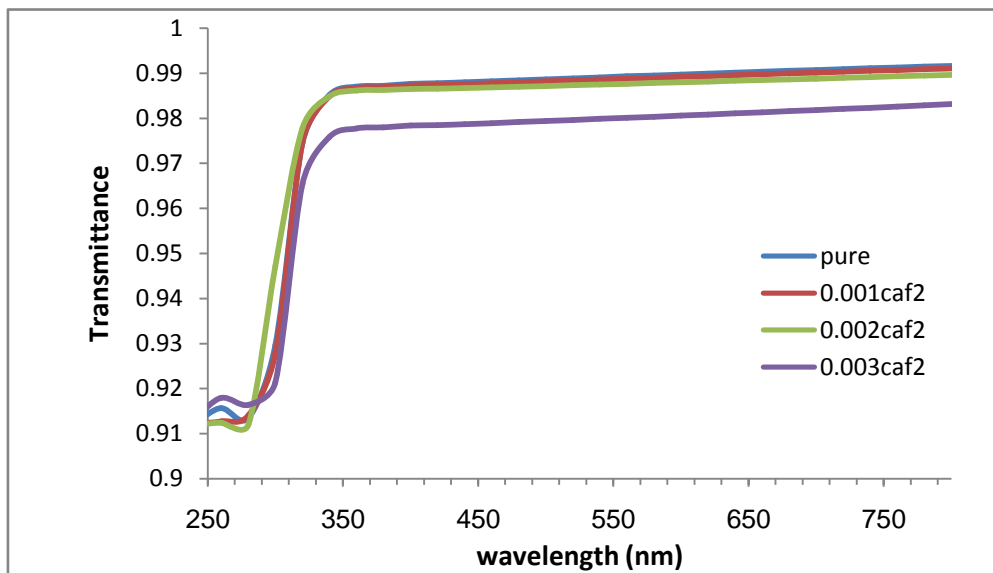


Figure 4. The transmittance versus wavelength of PVA- PAAm-PEG blend and PVA- PAAm-PEG: CNT nanocomposites.

Figure 5 The Extinction Coefficient (k_o) of PVA-PAAm-PEG:CNT nanocomposites with different concentrations of CNT is depicted in the figure, illustrating its variation with wavelengths. The extinction coefficient (k_o) was determined by applying Equation 2 [23]:

$$K_o = \alpha\lambda/4\pi \tag{2}$$

The figure shows that the extinction coefficient increases as the concentration of CNT in the PVA-PAAm-PEG nanocomposites rises. This can be attributed to increased optical absorption and photon scattering within the polymer matrix. Furthermore, the increase in extinction coefficient with wavelength can be explained by the constant absorption coefficient in the visible and near-infrared regions. As a consequence, there is a loss of resolution due to an increase in wavelength gradient [24].

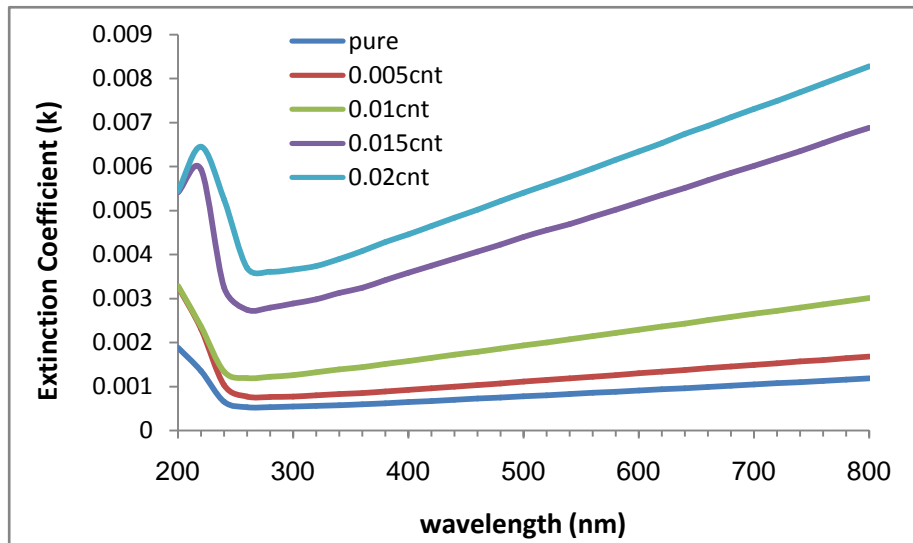


Figure 5. Variation of Extinction coefficient with wavelength of PVA- PAAm-PEG Blend and PVA- PAAm-PEG: CNT nanocomposites.

Figures 6 and 7 show the variation dielectric constant for two parts (real and imaginary) as a function of the wavelength. The dielectric constant for two parts (real and imaginary) has been calculated from equations 3 and 4 [25]:

$$\epsilon_1 = n^2 - k_0^2 \quad (3)$$

$$\epsilon_2 = 2nk_0 \quad (4)$$

The increase in both the real and imaginary parts of the dielectric constant is attributed to an enhanced electropolarization effect caused by a higher concentration of CNT in the sample. The figures show variations in the real and imaginary parts of the dielectric constant for both the PVA-PAAm-PEG blend and the PVA-PAAm-PEG:CNT nanocomposite at different wavelengths. This behavior can be explained by considering that the real part of the dielectric constant acts as a refractive index, particularly when there is minimal influence from the extinction coefficient. On the other hand, changes in the imaginary part of the dielectric constant are influenced by variations in extinction coefficient, especially within visible and near-infrared regions where there is relatively little change in refractive

index. The observed increase in extinction coefficient with wavelength contributes to these changes observed in the imaginary part of dielectric constant[26].

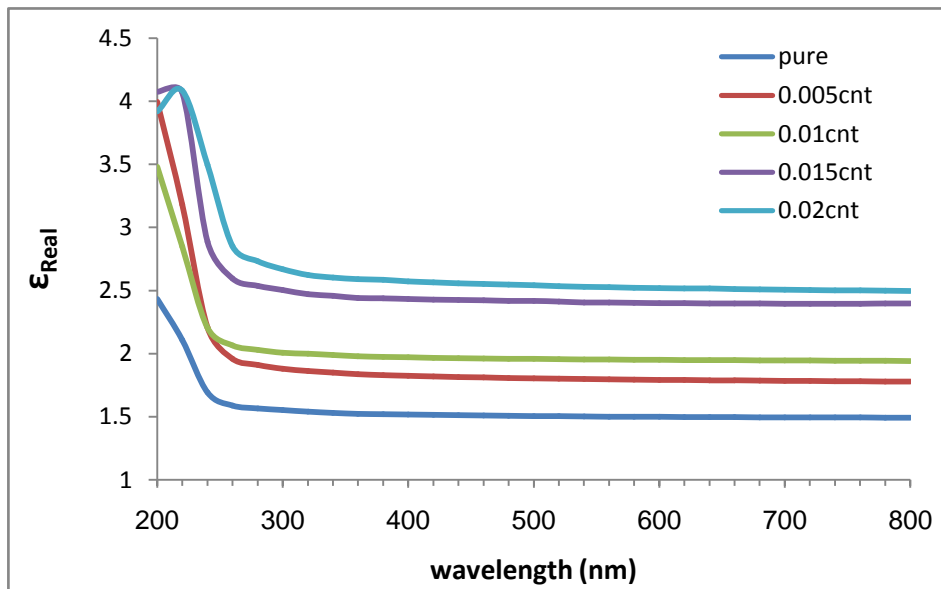


Figure 6. The real dielectric constant with the wavelength of PVA-PAAM-PEG blend and PVA- PAAM-PEG: CNT nanocomposite.

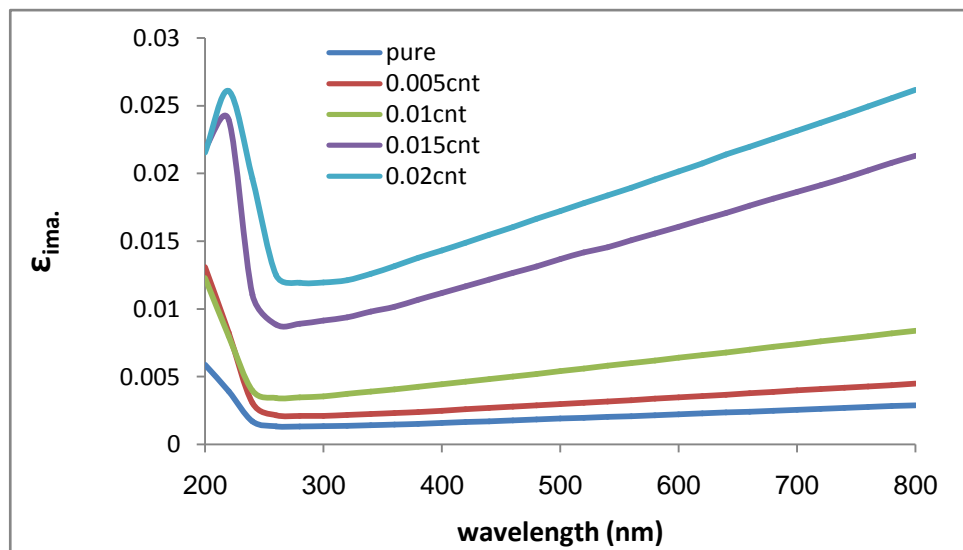


Figure 7. The real dielectric constant with the wavelength of PVA-PAAM-PEG blend and PVA- PAAM-PEG: CNT nanocomposite.

Dispersion Parameters

The Dispersion parameters were studied and diagnosed using the Wemple DiDomenico model. For PVA- PAAm-PEG: CNT nanocomposite are determined from the relation Wemple and DiDomenico [27]:

$$(n^2 - 1) = \frac{E_d E_0}{E_0^2 - (hv)^2} \quad (5)$$

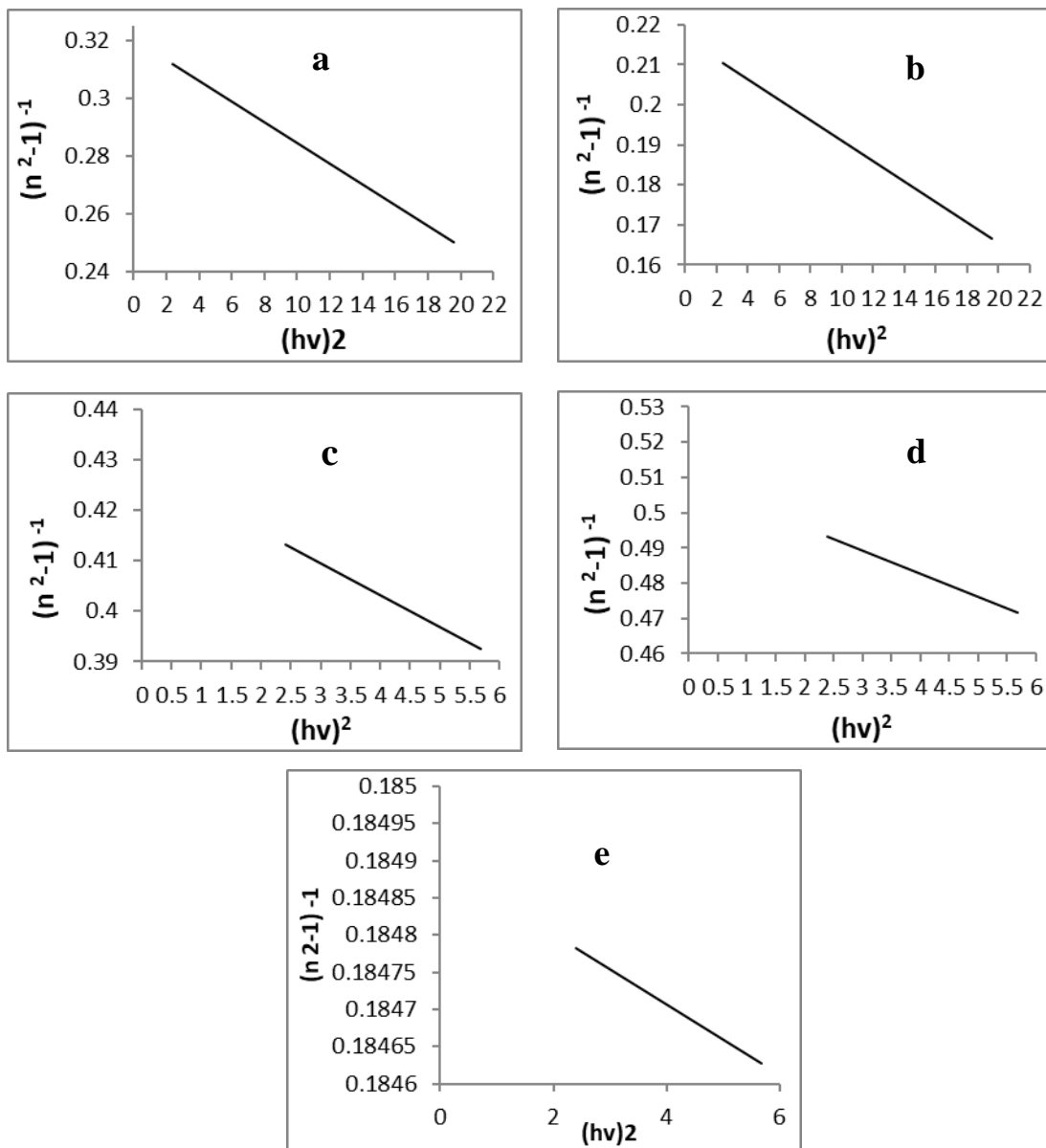
In the given equation, 'n' denotes the refractive index, 'E_o' stands for the oscillator strength, and 'E_d' represents the dispersion energy linked with the energy of optical transitions [28]. These coefficients can be obtained by plotting (n²-1)⁻¹ on the y-axis against (hv)² on the x-axis. Alternatively, the slope (E_o/E_d) and intercept (E_o/E_d) of the linear regression line can be used. Figure 8 demonstrates the relationship between (n²-1)⁻¹ and (hv)²[29].The resulting E_o and E_d parameters are summarized in Table 2. It was observed that both E_o and E_d values decreased with the increasing incorporation of CNT in the PAAm-PEG blend. Additionally, the bandgap (E_g) values can be approximated from the relationship E_o ≈ 2E_g [30].

The moments of the optical spectra (M₋₁, M₋₃) of PVA- PAAm-PEG: CNT can be determined using the following equations [31]:

$$E_0^2 = \frac{M_{-1}}{M_{-3}} \quad (6)$$

$$E_d^2 = \frac{M_{-1}^3}{M_{-3}} \quad (7)$$

The addition of CNTs to PVA-PAAm-PEG blends resulted in an increase in the optical spectral moments, as shown in Table 2. At the same time, there was a decrease in the energy difference values as the number of nanoparticles increased. Moreover, the augmentation of CNT nanoparticles resulted in increased values of n (0), M₋₁ and M₋₃ as depicted in Figure 8. These findings align with those reported by the previous researcher [32].



Figure(8): Plot of $(n^2 - 1)^{-1}$ vs $(hv)^2$ of PVA- PAAm-PEG-CNT with various content of CNT.

(a) 0 wt. (B) 0.005 wt. (c) 0.010 wt. (d) 0.015 wt. and (e) 0.020 wt.

Table 2. Optical parameters of PVA- PAAm-PEG: CNT nanocomposite.

parameter	PVA- PAAm-PEG				
	0 wt.	0.005 wt. CNT	0.010 wt. CNT	0.015 wt. CNT	0.020 wt. CNT
E_{O_2}	88.275	83.545	3	59.925	6
E_o	9.39547763		8.11993431	7.74112394	6.20036728
E_g	6	9.1402954	8	9	4
E_d	4.69773881		4.05996715	3.87056197	3.10018364
$n_{2(0)}$	8	4.5701477	9	5	2
$n_{o(0)}$	29.2694007	42.1211769	18.8835681	15.1786744	33.5336251
ϵ	3	6	8	1	2
M_{-1}	4.11526479	5.60829493	3.32558139	2.96078431	6.40832882
M_{-3}	8	1	5	4	6
	2.02861154	2.36818388	1.82361766	1.72069297	2.53146772
	4	9	7	5	2
	4.11526479	5.60829493	3.32558139	2.96078431	6.40832882
	8	1	5	4	6
	3.11526479	4.60829493	2.32558139	1.96078431	5.40832882
	8	1	5	4	6
	0.03529045	0.05515943		0.03272063	0.14067867
	4	4	0.03527171	9	1

Conclusions

PVA-PAAm-PEG:CNT blends were prepared using the injection method, and optical microscopy images revealed a uniform dispersion of the nanomaterial in the films. Scanning electron microscopy (SEM) was utilized to investigate the compatibility between different components of the polymers and nanomaterials, providing insights into the surface morphology of the PVA-PAAm-PEG:CNT nanocomposite films. XRD analysis confirmed the existence of semi-crystalline PVA-PAAm-PEG and aggregates, while also revealing the hexagonal structure of the CNT as the inclusion percentage increased up to 20wt.%. The transmission capacity decreased with higher concentrations of CNT. The extinction coefficient and dielectric constant exhibited an increase with increasing CNT concentration, which can be attributed to enhanced electrical polarization within the nanocomposite. This is a result of an increased number of charges in the polymer due to higher sample concentrations. Upon investigation of the scattering coefficients, it was observed that the augmentation of nanoparticles in the films led to a decrease in diffusion parameters such as E_o , E_d , $n(0)$, M_{-1} , M_{-3} , and ϵ . To assess the feasibility of utilizing the nanocomposites in optical devices, the Wemple-DiDomenico model was employed to ascertain these diffusion parameters.

References

- [1] M. E. Nicho, C. H. García-Escobar, M. C. Arenas, P (2011). Altuzar-Coello, R. Cruz-Silva, and M. Güizado-Rodríguez, "Influence of P3HT concentration on morphological, optical and electrical properties of P3HT/PS and P3HT/PMMA binary blends," *Mater. Sci. Eng. B*, 176, 17.
- [2] X. Wang, C. G. Bazuin, and C (2015). Pellerin, "Effect of small molecule hydrogen-bond crosslinker and solvent power on the electrospinnability of poly (4-vinyl pyridine)," *Polymer (Guildf)*, 57, 62–69.

- [3] I. Vinckier, H.M Laun, (2000). "Manifestation of spinodal decomposition in oscillatory shear measurement", *Macromol. Symp.*, 149, 151–156.
- [4] S. Uslu, A. Keskin, T.C Gul,. M.L Karabulut, (2010). "Aksu, Preparation and properties of electrospun poly (vinyl alcohol) blended hybrid polymer with aloe vera and HPMC as wound dressing. Hacet". *J. Biol. Chem.* 38(1), 19–25.
- [5] B. Ben Doudou, A. Vivet, J. Chen, A. Laachachi, T. Falher, and C (2014). Poilâne, "Hybrid carbon nanotube—silica/polyvinyl alcohol nanocomposites films: preparation and characterisation," *J. Polym. Res.*,21, 4,1–9.
- [6] A. Gautam and S (2010). Ram, "Preparation and thermomechanical properties of Ag-PVA nanocomposite films," *Mater. Chem. Phys.*,119,1–2,266–271.
- [7] K. H. Abass and H. A. Hamed, (2020). "Reduction of Energy Gap in ZrO₂ Nanoparticles on Structural and Optical Properties of Casted PVA–PAAm Blend", *Journal of Green Engineering*,10,7, 4166–4176.
- [8] RJ. Young, M. Liu, IA. Kinloch, et al (2018). "The mechanics of reinforcement of polymers by graphene nanoplatelets". *Compos Sci Technol* 154:110–116.
- [9]. LA, Kolahalam, IV. K. Viswanath, BS. Diwakar, et al (2019) Review on nanomaterials: Synthesis and applications. *Mater Today Proc* 18:2182–2190.
- [10]. A.N.Al-Jamal, Q.M. Hadi, F.J. Hamood, K.H. Abass, (2019). "Particle size effect of Sn on structure and optical properties of PVA-PEG blend", *Proceedings - International Conference on Developments in eSystems Engineering*, DeSE,736-740.
- [11]. SS. Devangamath, B. Lobo, SP. Masti, et al. (2020)," Thermal, mechanical, and AC electrical studies of PVA–PEG–Ag₂S polymer hybrid material", *Journal Mater Sci Mater Electron* 31: 2904–2917.
- [12] K. H. Abass, A. M. Kadim, S. K. Mohammed, M. A. Agam, (2021). "Drug Delivery Systems Based on Polymeric Blend: A Review", *Nano Biomed. Eng.*13(4),414-424.

- [13]. A-KJ Rashid, ED. Jawad, BY. Kadem, (2011), A study of some mechanical properties of Iraqi palm fiber-PVA composite by ultrasonic, Eur J Sci Res 61: 203–209.
- [14] R. Klein, “Laser Welding of Plastics”, John Wiley and Sons. (2012).
- [15] S. Amin, and M (2011). Amin, “Thermoplastic Elastomeric (Tpe) Materials and Their Use in Outdoor Electrical Insulation”, Rev. Adv. Mater. Sci.29,15-30.
- [16] J. M. G (1991). Cowie, “Polymers: Chemistry and Physics of Modern Materials”, Glasgow.
- [17] J. J. Scobbo, and L. A (2003). Goettler, “Applications of polymer alloys and blends”, Kluwer Academic Publishers.
- [18] Y. M. Yue, K. Xu, X. G. Liu, Q. Chen, X. Sheng, and P. X. Wang (2008). “Preparation and characterization of interpenetration polymer network films based on poly (vinyl alcohol) and poly (acrylic acid) for drug delivery”, Journal of applied polymer science, 108(6),3836-3842.
- [19] Abass, K.H., Hataf, A.H., Mubarak, T.H., "Effect of Ag nanoparticles on AC electrical parameters of PVA-PAAm and PVA-PMMA-PAAm blends", AIP Conference Proceedings [this link is disabled](#), 2023, 2475, 090036.
- [20] h. G. Yang, N. N. Liu., S. Dong., F. S. Tian, Y. Gao, Z. Hou (2019). “Supercapacitors based on free-standing reduced graphene oxides/ carbon nanotubes hybrid flms”, SN Applied Sciences.
- [21] C. Kittel ,(1981). “Introduction to solid state physics”, 5th Ed, Willy, New York.
- [22] A.S. Alkelaby, K.H. Abass, T.H. Mubarak, N.F. Habubi, S.S. Chiad, I. Al-Baidhany, (2019). "Effect of MnCl₂ additive on optical and dispersion parameters of poly methyl methacrylate films", Journal of Global Pharma Technology 11(4), 347-352.

- [23] N. Mahfoudh, K. Karoui , A. BenRhaïem, (2021). “Optical studies and dielectric response of $[\text{DMA}]_2\text{MCl}_4$ (M = Zn and Co) and $[\text{DMA}]_2\text{ZnBr}_4$. RSC advances”,11(40): 24526-24535.
- [24] N.H. Abdali, S.H. Al-Rubaye, B.H.Rabee, K.H. Abass, (2021). "Electrochemical Performance Enhancement Zinc Cobaltite-Reduced Graphene Oxide for Next Generation Energy Storage Applications", Journal of Physics: Conference Series,1818(1).
- [25] K. H. Abass and O. Haidar, (2019), "0.006wt.%Ag-Doped Sb_2O_3 Nanofilms with Various Thickness: Morphological and optical properties", Journal of Physics: Conference Series, 1294(2),
- [26] R. G Kadhim, (2016). “Study of Some Optical Properties of Polystyrene-Copper Nanocomposite Films”, World Scientific News,30,14.
- [27] S. H Wemple and M. DiDomenico, (1971). “Behavior of the electronic dielectric constant in covalent and ionic materials,” Phys. Rev. B, 3, 4, 1338–1351.
- [28] K.S. Sharba, A.S. Alkelaby, M.D. Sakhil, K.H. Abass, N.F. Habubi, S.S. Chiad (2020). “Enhancement of urbach energy and dispersion parameters of polyvinyl alcohol with Kaolin additive”. NeuroQuantology; 18(3): 66-73.
- [30] Mohammed, H.R.A., Al-Ogaili, A.O.M., Abass, K.H., "Structural and dispersion parameters of nano-layers prepared from Al-Ni-Cr alloy", Materials Today: Proceedings, 2023, 80, pp. 2396-3304.
- [31] A.K. Walton, T.S. Moss (1963). “Determination of refractive index and correction to effective electron mass in PbTe and PbSe”. Proceedings of the Physical Society, 81(3): 1958-1967.
- [32] A. A. K. Zbala, A. O. Mousa Al-Ogaili, Khalid HaneenAbass, (2022),” Optical Properties and Dispersion Parameters of PAAm-PEG Polymer Blend Doped with Antimony (III) Oxide Nanoparticles”, NeuroQuantology, 20 (2) 62-68